water

Article

Long-Term Variability of the Hydrological Regime and Its Response to Climate Warming in the Zhizdra River Basin of the Eastern European Plain

Bing Bai [1,2], Qiwei Huang [1,2], Ping Wang [1,2], Shiqi Liu [1], Yichi Zhang [1,*], Tianye Wang [3], Sergey P. Pozdniakov [4], Natalia L. Frolova [5] and Jingjie Yu [1]

1 Key Laboratory of Water Cycle and Related Land Surface Processes, Institute of Geographic Sciences and Natural Resources Research, Chinese Academy of Sciences, 11A, Datun Road, Chaoyang District, Beijing 100101, China; baibing22@mails.ucas.ac.cn (B.B.); huangqw.19s@igsnrr.ac.cn (Q.H.); wangping@igsnrr.ac.cn (P.W.); liusq@igsnrr.ac.cn (S.L.); yujj@igsnrr.ac.cn (J.Y.)
2 University of Chinese Academy of Sciences, Beijing 100049, China
3 School of Water Conservancy Engineering, Zhengzhou University, 100 Science Avenue, Zhengzhou 450001, China; wangtianye@zzu.edu.cn
4 Department of Hydrogeology, Lomonosov Moscow State University, GSP-1, Leninskie Gory, Moscow 119899, Russia; sppozd@mail.ru
5 Department of Land Hydrology, Lomonosov Moscow State University, GSP-1, Leninskie Gory, Moscow 119991, Russia; frolova_nl@mail.ru
* Correspondence: zhangych@lreis.ac.cn

Abstract: Climate warming globally has a profound effect on the hydrological regime, amplifying evapotranspiration and precipitation and accelerating the processes of snow melt and permafrost thaw. However, in the context of small river basins—those encompassing less than 10,000 km^2—the response of the hydrological regime to climate change is intricate and has not yet been thoroughly understood. In this study, the Zhizdra River Basin, a typical small river basin in the eastern European plain with a total drainage area of 6940 km^2, was selected to investigate the long-term variability of the hydrological regime and its responses to climate warming. Our results show that during the period of 1958–2016, the average runoff in the Zhizdra River Basin was approximately 170 mm, with significant fluctuations but no trend. Sensitivity analysis by the Budyko framework revealed that the runoff was more sensitive to changes in precipitation (P) compared to potential evapotranspiration (E_0), implying that the Zhizdra River Basin is limited by water availability and has a slightly dry trend. A comprehensive analysis based on the seasonality of hydrometeorological data revealed that temperature predominantly affects spring runoff, while P mainly controls autumn runoff. Both factors make significant contributions to winter runoff. In response to climate change, the nonuniformity coefficient (C_v) and concentration ratio (C_n) of runoff have noticeably declined, indicating a more stabilized and evenly distributed runoff within the basin. The insights gleaned from this research illuminate the complex hydrological responses of small river basins to climate change, underlining the intricate interrelation among evapotranspiration, precipitation, and runoff. This understanding is pivotal for efficient water resource management and sustainable development in the era of global warming.

Keywords: hydrological regime; precipitation; evapotranspiration; climate change; Budyko framework

check for updates

Citation: Bai, B.; Huang, Q.; Wang, P.; Liu, S.; Zhang, Y.; Wang, T.; Pozdniakov, S.P.; Frolova, N.L.; Yu, J. Long-Term Variability of the Hydrological Regime and Its Response to Climate Warming in the Zhizdra River Basin of the Eastern European Plain. *Water* **2023**, *15*, 2678. https://doi.org/10.3390/w15152678

Academic Editors: Jianhua Xu and Zhongsheng Chen

Received: 30 June 2023
Revised: 22 July 2023
Accepted: 23 July 2023
Published: 25 July 2023

1. Introduction

Runoff is a vital component of the water cycle [1]. Approximately 24% of the world's rivers experience significant variations in water flux, with changes in flow determined by climate factors such as temperature, evapotranspiration, and precipitation [2,3]. The variability in regional runoff resources due to climate change poses a significant threat to sustainable development in affected areas [4]. Understanding the trends in runoff and comprehending the underlying reasons behind these changes have become crucial challenges in the face of complex and ever-changing hydroclimatic conditions [5].

While precipitation and evapotranspiration are traditionally considered as key drivers of runoff changes [6], recent studies have revealed the significant influence of other factors, such as wildfires [7], seasonal climate variations [8,9], seasonal snowmelt [10], permafrost degradation [11–13], and human activities [14]. To assess the impact of these driving factors on changes in runoff, various quantitative methods and models have been developed.

Hydrological models such as SWAT, physically based glacier hydrological models, and assimilation-based stochastic hydrological simulation systems have been widely employed to estimate runoff contributions [15–19]. However, these models often face challenges related to computational costs, parameter estimation, sensitivity, and result uncertainty [20,21]. Conceptual models such as the Budyko model offer potential advantages in capturing hydrological processes while requiring fewer data [22–24].

It has been documented that more than 30% of the small tributaries that replenished the Oka River Basin have ceased to exist over the past 60 years [25]. Therefore, the Zhizdra River Basin, one of the three major tributaries of the Oka River, located in the central part of the East European Plain in European Russia, were selected in this study. With relatively low human activity in the basin, it provides an excellent opportunity to investigate the impact of climate change on runoff. Understanding the current climate change's effects on water resources is crucial for effective water management measures in Russia [26,27]. The objectives of this study were to: (1) examine the long-term variability of the hydrological regime in the Zhizdra River Basin from 1958 to 2016; (2) quantify the contribution of predominant climate factors to runoff changes using the Choudhury–Yang equation based on the Budyko hypothesis; and (3) assess the effects of precipitation and potential evapotranspiration on runoff in different seasons. By addressing these objectives, this research aims to enhance our understanding of the hydrological processes in the Zhizdra River Basin and provide valuable information for water resource management.

2. Materials and Methods

2.1. Study Area

The Zhizdra River Basin (54.0°–54.2° N, 34.9°–35.6° E) was selected to analyse the variability in runoff from 1958 to 2016 (Figure 1). With an area of approximately 6940 km^2, the basin qualifies as a small-scale basin [28]. The runoff of the Zhizdra River is composed of three parts, namely snowmelt, rainfall, and groundwater runoff [29]. The runoff is much greater in spring and winter than in summer and autumn.

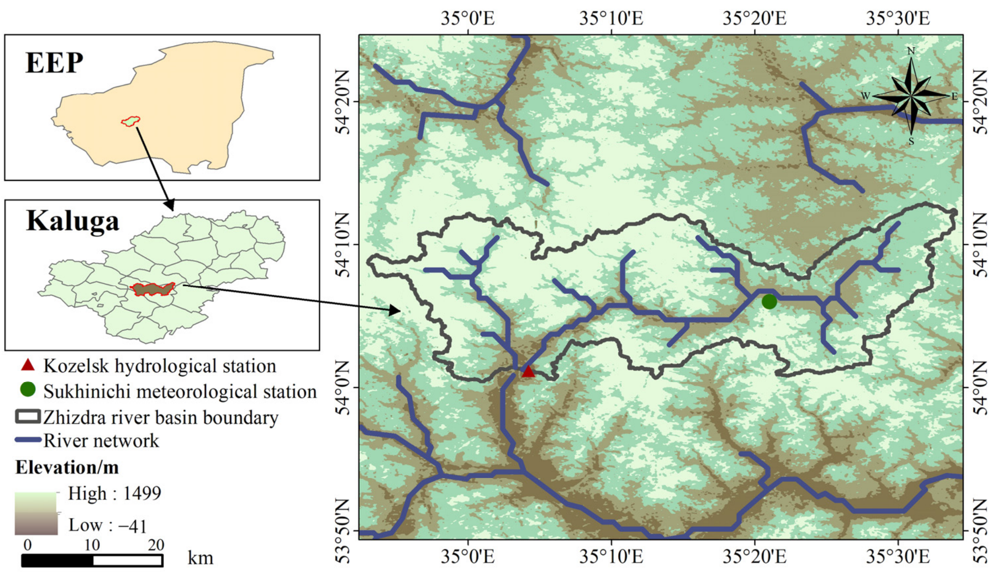

Figure 1. Geographic location of the Zhizdra River Basin (EEP refers to the East European Plain).

The Zhizdra River belongs to the central part of the East European Plain, with a moderately continental climate. In summer and autumn, the evapotranspiration in the Zhizdra is high. In winter, Zhizdra is covered with layers of snow, and the snow period of the year lasts 5.7 months, from October to April. The Zhizdra River Basin is characterized by a low population density, where approximately 50% of the land is dedicated to agricultural use. Additionally, a substantial portion of the basin is classified as an agricultural geo-ecological region, with minimal industrial activity [30]. The Zhizdra is subject to minimal human disturbance, with no large centralized groundwater extraction points or water management structures regulating river flow within the basin [31]. As such, it represents a natural setting for analysing the impact of climate change on small watershed runoff. The downstream area of the Zhizdra River is Ugra National Park. In 2002, it was designated a biosphere reserve by UNESCO. As such, changes in runoff are closely linked to downstream ecological conditions.

2.2. Data

The daily runoff data used in this study were obtained from Pozdniakov, et al. [32] and cover the period from 1958 to 2016. The data were obtained from ground-based hydrological stations. Runoff measurements are subject to various sources of uncertainty, including wind effects, ice presence, boundary influences, flow obstructions, improper equipment, incorrect measuring procedures, and human errors, which can contribute to standard errors ranging from 3% to 6% [33]. Over the past fifty years, the measurement techniques, equipment, and flow computation methods in Russia have not undergone significant changes. Climate data, including temperature, precipitation, potential evapotranspiration, and total evapotranspiration, were obtained from the ERA5 dataset, specifically the ERA5-Land monthly averaged data from 1950 to present [34], and cover the period from 1958 to 2016 (URL: https://doi.org/10.24381/cds.68d2bb30 (accessed on 24 September 2022)) [35]. All data were carefully checked for errors and gaps, and no missing values were identified.

2.3. Mann–Kendall Trend Test

The Mann–Kendall trend test is a common method used in the fields of meteorology and hydrology. It is a nonparametric statistical method, and the data may not be normally distributed. Therefore, it applies to hydrometeorological data including discharge, temperature, and precipitation series. Suppose X_1, $X_2 \ldots$, X_n are the time-series variables, and n is the length of the time series. The M-K test defines the statistic S:

$$S = \sum_{j=1}^{n-1} \sum_{k=j+1}^{n} sgn\left(X_k - X_j\right) \tag{1}$$

$$sgn\left(X_k - X_j\right) = \begin{cases} 1, X_k - X_j > 0 \\ 0, X_k - X_j = 0 \\ -1, X_k - X_j < 0 \end{cases} \tag{2}$$

where X_j and X_k are the values of years j and k, respectively, and $k > j$.

$$Z = \begin{cases} \frac{S-1}{\sqrt{Var(S)}}, S > 0 \\ 0, S = 0 \\ \frac{S+1}{\sqrt{Var(S)}}, S < 0 \end{cases} \tag{3}$$

where Z is a statistic of normal distribution, and $Var(S)$ is variance. At a given α confidence level, if $|Z| \geq Z_{1-\alpha/2}$, the null hypothesis is rejected; that is, the time series have an obvious upwards or downwards trend. Z represents a positive value indicating an upward trend and a negative value indicating a decreasing trend. The absolute value of Z, when greater than 1.645, 1.96, and 2.576, indicates significance at the 90%, 95%, and 99% confidence levels, respectively.

2.4. Sliding t-Test

The sliding *t*-test is a statistical method used to assess the significance of the difference between the average values of two groups of samples. The underlying concept involves comparing the mean values of two series from the same climate series like comparing the mean values of two populations. If the observed differences exceeds a predetermined level of significance, it indicates a change point [36].

$$t = \frac{\overline{x_1} - \overline{x_2}}{S \cdot \sqrt{\frac{1}{n_1} + \frac{1}{n_2}}} \tag{4}$$

$$S = \sqrt{\frac{n_1 s_1^2 + n_2 s_2^2}{n_{1+} n_2 - 2}} \tag{5}$$

The time series x is divided into two series, x_1 and x_2. n_1 and n_2 are the sample sizes of x_1 and x_2. The mean values of the two series are $\overline{x_1}$ and $\overline{x_2}$, and the variances are s_1^2 and s_2^2. The t statistic follows a t-distribution with degrees of freedom equal to $n_1 + n_2 - 2$. The reference point is set by sliding (artificially set the step size), and the t statistic is calculated in turn (Equation (4)). When a significance level of α is given, a mutation occurs if $|t_i| > t_\alpha$, and it can be concluded that there is a significant difference between the means of the two populations [37].

We set the step size to 5 because a smaller size allows for a more detailed analysis [38] and provides higher resolution and increased sensitivity in detecting change points [39].

2.5. Nonuniformity Index of Intra-Annual Runoff

Based on daily runoff data, we calculated the nonuniformity coefficient of annual runoff distribution. A higher C_v indicates a greater difference in monthly runoff in a year and a more nonuniform distribution of runoff in a year [40,41]. C_v can be expressed as follows:

$$C_v = \frac{\sigma}{R} \tag{6}$$

$$\sigma = \sqrt{\frac{\sum_{i=1}^{12} (R_i - R)^2}{12}} \tag{7}$$

$$R = \frac{\sum_{i=1}^{12} R_i}{12} \tag{8}$$

where R_i is the monthly runoff in the year, R is monthly average runoff in the year, i is the month, and σ is the standard deviation.

The runoff concentration ratio (C_n) serves as an indicator of the level of concentration within the intra-annual runoff distribution. A higher C_n denotes an elevated degree of instability and fluctuation in the characteristics of intra-annual runoff distribution [41,42]. We regard the runoff of each month in a year as a vector, the value is the length of the vector, and the month is the direction of the vector. The azimuth θ of each month from January to December is 0°, 30°, 60°, . . ., 360°, decomposing the monthly runoff in the x and y directions. Then, the vector synthesis in the x and y directions is as follows:

$$R_x = \sum_{i=1}^{12} R_i cos\theta_i \tag{9}$$

$$R_y = \sum_{i=1}^{12} R_i sin\theta_i \tag{10}$$

The synthesis of runoff is as follows:

$$R = \sqrt{{R_x}^2 + {R_y}^2} \tag{11}$$

C_n can be calculated as given:

$$C_n = R / \sum_{i=1}^{12} R_i \tag{12}$$

C_n indicates the ratio of the runoff in the direction of the synthetic vector of monthly runoff to the annual runoff. Therefore, there is a clear correlation between C_n and the ratio of flood season runoff to annual runoff.

2.6. Sensitivity of Runoff to Climate Change

Due to its accurate and concise representation of the relationship between annual evapotranspiration and long-term-average water and energy balance at catchment scales, the Budyko equation has achieved iconic status in hydrology [43,44]. A frequent application of parametric models of the Budyko equation has been to estimate the climate elasticity to predict the effects of changes in precipitation (P) and potential evapotranspiration (E_0) on catchment evapotranspiration and, therefore, runoff [45]. Evapotranspiration (E) and runoff (Q) can be calculated as a function of P, E_0, and a parameter that describes basin properties (n) [23]. We mainly used the Choudhury–Yang equation, also known as the generalized Budyko equation.

$$E = \frac{PE_0}{\left(P^n + E_0^n\right)^{1/n}} \tag{13}$$

The change in E can be expressed by the change in P, E_0, and n.

$$dE = \frac{\vartheta E}{\vartheta P} dP + \frac{\vartheta E}{\vartheta E_0} dE_0 + \frac{\vartheta E}{\vartheta n} dn \tag{14}$$

with the respective partial differentials provided as follows:

$$\frac{\vartheta E}{\vartheta P} = \frac{E}{P}\left(\frac{E_0^n}{P^n + E_0^n}\right) \tag{15}$$

$$\frac{\vartheta E}{\vartheta E_0} = \frac{E}{E_0}\left(\frac{P^n}{P^n + E_0^n}\right) \tag{16}$$

$$\frac{\vartheta E}{\vartheta n} = \frac{E}{n}\left(\frac{ln\left(P^n + E_0^n\right)}{n} - \frac{\left(P^n lnP + E_0^n lnE_0\right)}{P^n + E_0^n}\right) \tag{17}$$

Assume a steady-state water balance for the basin in this study. These equations express how Q is affected by climate factors and basin properties:

$$\frac{dQ}{Q} = \left[\frac{P}{Q}\left(1 - \frac{\vartheta E}{\vartheta P}\right)\right]\frac{dP}{P} - \left[\frac{E_0}{Q}\frac{\vartheta E}{\vartheta E_0}\right]\frac{dE_0}{E_0} - \left[\frac{n}{Q}\frac{\vartheta E}{\vartheta n}\right]\frac{dn}{n} = \varepsilon P\frac{dP}{P} - \varepsilon E_0\frac{dE_0}{E_0} - \varepsilon n\frac{dn}{n} \tag{18}$$

where ε_P, ε_{E0}, and ε_n are the sensitivity coefficients of P, E_0, and n to Q, respectively.

3. Results

3.1. Temporal Changes in Climate

From 1958 to 2016, the annual average temperature (T) of the Zhizdra River Basin was 5.35 °C, with a highest temperature in summer (June to August) of 25 °C and lowest in winter (December to February) of approximately −17 °C. Over this period, the annual average temperature has experienced a continuous increase ($p < 0.01$), rising by 0.3 °C/10a

(Figure 2a) (10a denotes a period of 10 years). After 2000, temperature fluctuations have gradually decreased, and the temperature has risen steadily.

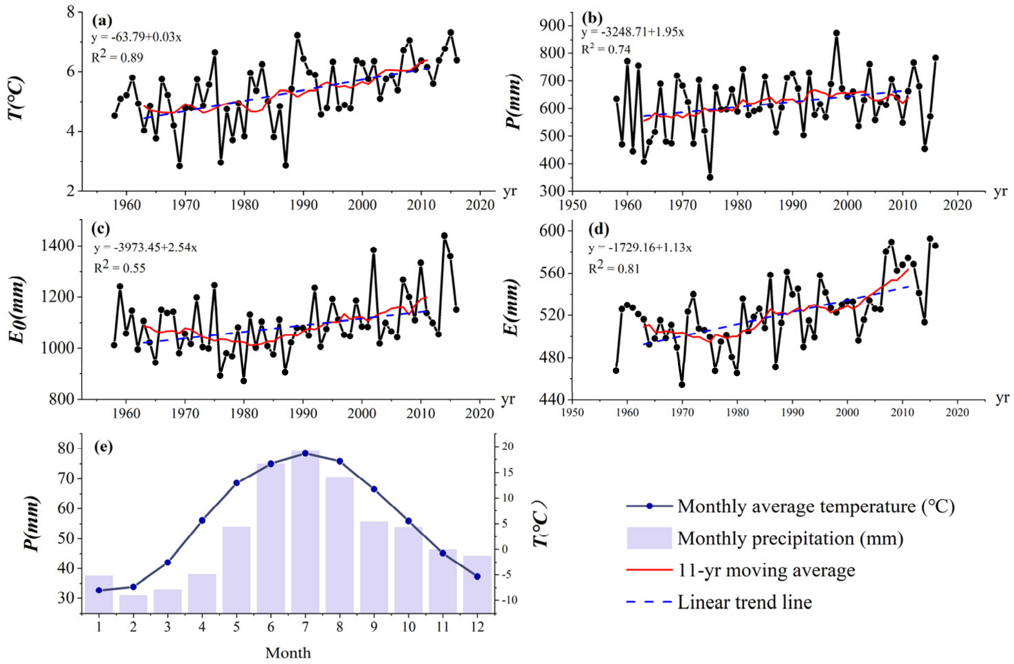

Figure 2. Time series of (**a**) precipitation (P), (**b**) temperature (T), (**c**) potential evapotranspiration (E_0), and (**d**) evapotranspiration (E). The time series for (**a**–**d**) spans 1958 to 2016. The black solid line represents the annual average value of meteorological elements. (**e**) The monthly average temperature and precipitation in the Zhizdra River Basin from 1958 to 2016.

During the period from 1958 to 2016, the annual average precipitation (P) in the basin was approximately 618 mm, with the highest amounts recorded during summer (225 mm) followed by autumn (September to November), with relatively less precipitation (<125 mm) in spring (March to May) and winter (Figure 2e). The 1990s was the wettest decade in the Zhizdra River Basin from 1958–2016, with an average precipitation of 663 mm (Figure 2b), which increased by 19.5 mm/10a.

The annual average potential evapotranspiration (E_0) in the Zhizdra River Basin was as high as 1094 mm from 1958–2016, with the annual evapotranspiration (E) around 523 mm. There was a significant increase in both E_0 and E: by 25.4 mm/10a ($p < 0.01$) and 11.3 mm/10a ($p < 0.01$), respectively (Figure 2c,d).

3.2. Temporal Changes in Runoff

The annual runoff within the Zhizdra River Basin has been recorded at approximately 170 mm, exhibiting a considerable fluctuation but without a distinct trend from 1958 to 2016, as depicted in Figure 3a. The annual runoff reached its peak in 1971, registering 307.8 mm, while the minimum annual runoff occurred in 2015 (93.8 mm) with the largest annual E. As shown in Figure 3b, runoff varies seasonally, with higher values during spring and lower values in the other seasons. The peak runoff occurs in April, with an average runoff depth of 57 mm. Conversely, the monthly average runoff is relatively low (approximately 9 mm) spanning from June through February, with August bearing the lowest monthly runoff at around 7 mm. Both summer and autumn runoff account for 15% each of the annual runoff, whereas spring and winter constitute 54% and 16%, respectively. The Mann–Kendall (MK) trend test suggests a significant increase ($p < 0.01$) in the summer and winter runoff from 1958 to 2016.

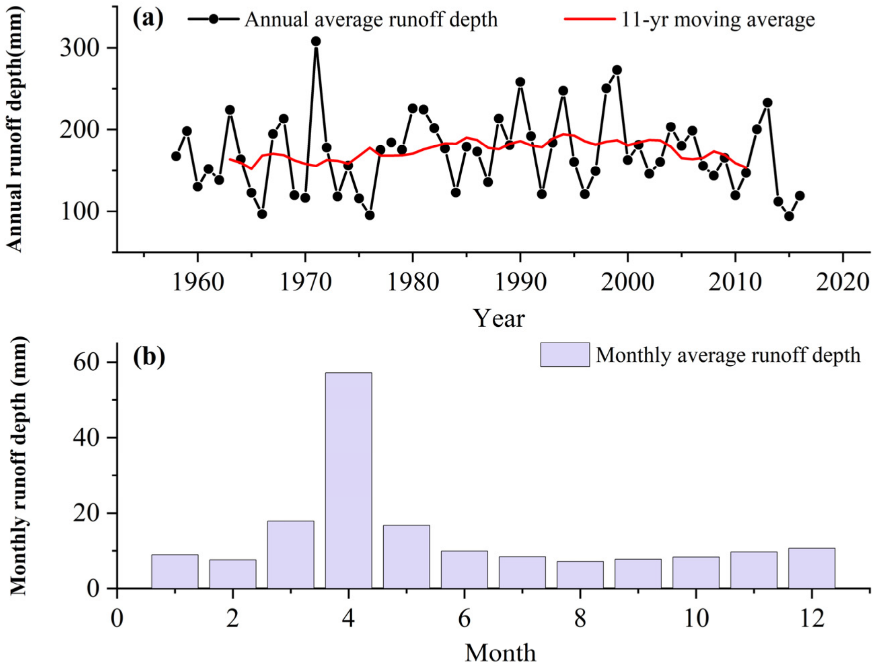

Figure 3. (**a**) Annual average runoff depth (mm) and 11-year moving average for the Zhizdra River Basin from 1958 to 2016 and (**b**) monthly average runoff depth (mm) for 1958–2016 in the Zhizdra River Basin.

Figure 4 depicts the variations in the nonuniformity coefficient (C_v) and concentration ratio (C_n) associated with annual runoff. The maximum value of C_v was 2.27 in 1968, while the minimum was 0.16 in 2015 (Figure 4a). The C_v showed a significant decrease trend ($p < 0.01$), indicating that the annual runoff distribution tended to be more uniform. The concentration ratio (C_n), which was predominantly between 20% and 55% from 1958 to 2016, experienced a low of 1.5% in 1991 and a high of 78.1% in 1968 (Figure 4b). A notable decrease in C_n ($p < 0.05$) suggests reduced concentration in annual runoff. A strong correlation of 0.87 ($p < 0.01$) was found between C_n and C_v, as determined by a Pearson two-tailed test, enhancing the reliability of the concentration assessments. The declining trend in both C_n and C_v implies diminished annual runoff fluctuation and increased stability.

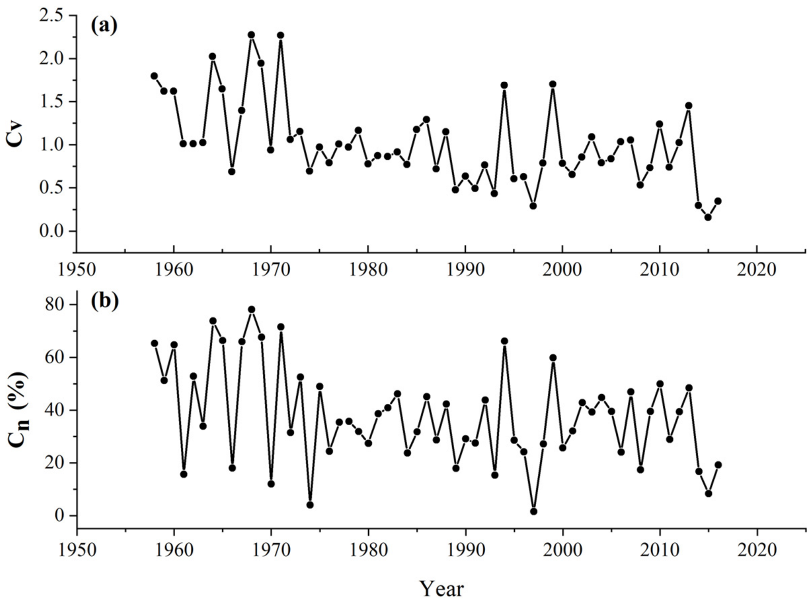

Figure 4. Nonuniformity index (**a**) and concentration ratio (**b**) of the annual runoff distribution.

To analyse the changing trends and identify the year of abrupt change, we employed a sliding t-test with a 5-year step size. Significant changes of runoff could be found in 1982 and 1977, with the absolute t-value exceeding 2.306 based on the t-test result of Q (Figure 5a). The negative t-value for 1977 suggests a notable decrease in Q ($p < 0.05$). Notably, T and E_0 significantly dropped in 1976 and 1973, which were values close to those in 1977 (Figure 5b,c). Conversely, the positive t-value in 1982 implies a substantial rise in Q ($p < 0.05$). T increased significantly in 1983 and was close to that in 1982. In 1996, both T and E decreased significantly (Figure 5d). It is worth noting that P did not display any significant changes over the 59-year period (Figure 5e).

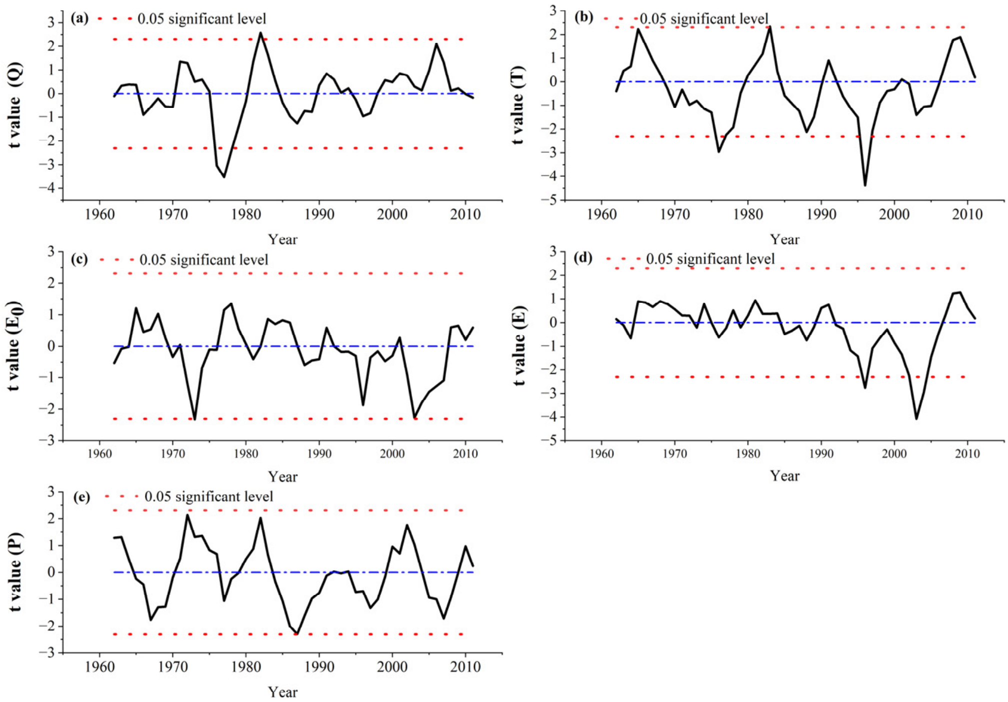

Figure 5. Sliding t-test for (**a**) runoff (Q), (**b**) temperature (T), (**c**) potential evapotranspiration (E_0), (**d**) evapotranspiration (E), and (**e**) precipitation (P). The time series spans 1958 to 2016. The red line represents 0.05 significance level. The blue line represents the t-value of 0.

3.3. Potential Impact of Climate Changes on Runoff

Assuming that, from 1958 to 2016, the watershed changed from one steady state to another, where any transient changes in storage were negligible, then the change in Q is calculated as: $dQ = dP - dE$. The parameter values required for Equations (15)–(17) can be found in Table 1. According to Equation (14), changes in E due to changes in climate and basin properties are calculated as follows:

$$dE = 0.486dP + 0.133dE_0 + 186.227dn \tag{19}$$

Table 1. Climatic Variables and Sensitivity Coefficients in Three Periods.

Period	P, mm	E_0, mm	Q, mm	n	ε_p	ε_{E0}	ε_n
1958–2016	618	1102	170	1.232	1.861	−0.861	1.346
1958–1977	573	1066	159	1.197	1.839	−0.839	1.367
1978–2016	642	1158	173	1.263	1.880	−0.880	1.330

The change in E with respect to P (0.486) is more sensitive than E_0 (0.133). This means that E is controlled by water availability. The change in Q is as given:

$$\frac{dQ}{Q} = 1.861\frac{dP}{P} - 0.861\frac{dE_0}{E_0} - 1.346\frac{dn}{n} \tag{20}$$

Change in Q with respect to P is more sensitive than the corresponding change in E_0, and a 10% increase in P resulted in an increase in Q of approximately 19%, while a 10% increase in E_0 will lead to a 9% decrease in Q. To further analyse the impact of each factor on runoff over time, we divided the period into two sequences: 1958–1977 and 1977–2016; not only did Q have a sudden change in 1977, but T and E_0 also had a sudden change in the 1970s. The sensitivity coefficients are shown in Table 1. From 1958 to 2016, Q was found to be increasingly sensitive to P, and this sensitivity has become more prominent since 1977. Specifically, after 1977, P increased by 10%, and Q increased by 0.4% compared to before. Moreover, the n value exhibited an increasing trend from 1.197 to 1.263 (Table 1).

Under the same aridity ratio (E_0/P), with a decrease in n, the evapotranspiration ratio (E/P) also decreases (Figure 6). The value of n increased slightly after 1977, which means that E/P will increase, and E will increase in the Zhizdra River Basin under the condition of constant precipitation. Considering the water balance equation ($Q = P - E$), the runoff will decrease. This means that after 1977, the water regime was more limited by the availability of water.

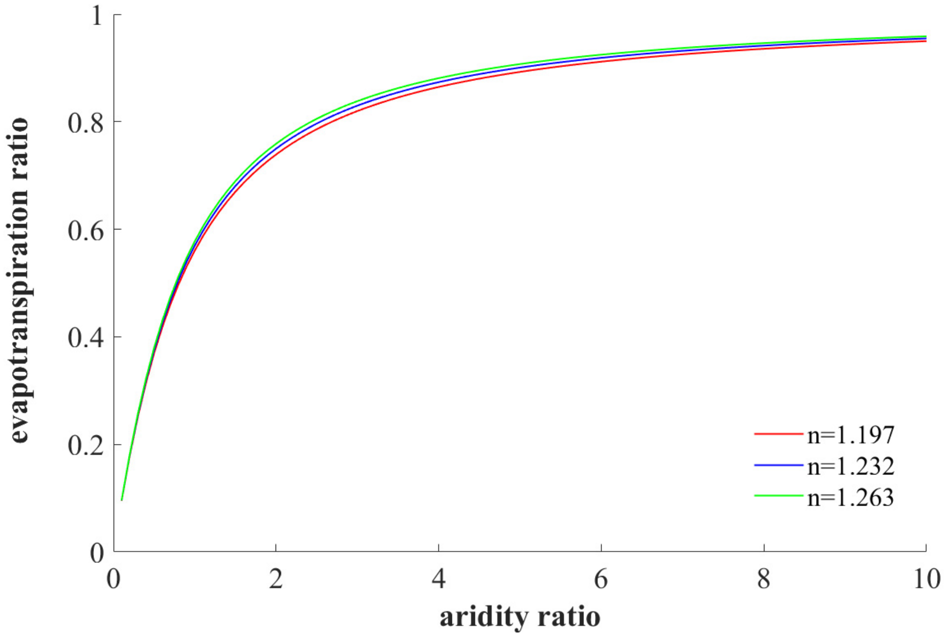

Figure 6. Relationships among the aridity ratio, evapotranspiration index, and underlying surface parameter (n).

In order to further study the influence of precipitation and potential evapotranspiration on runoff in Zhizdra River Basin in different seasons, according to the methods of Risbey and Entekhabi [46], Fu, et al. [47], and Wang, et al. [48], we calculated runoff ($\Delta Q = \frac{Q-\overline{Q}}{\overline{Q}}$), precipitation ($\Delta P = \frac{P-\overline{P}}{\overline{P}}$), and potential evapotranspiration ($\Delta E_0 = \frac{E_0-\overline{E_0}}{\overline{E_0}}$) and plotted the results on the precipitation-potential evapotranspiration plane (Figure 7).

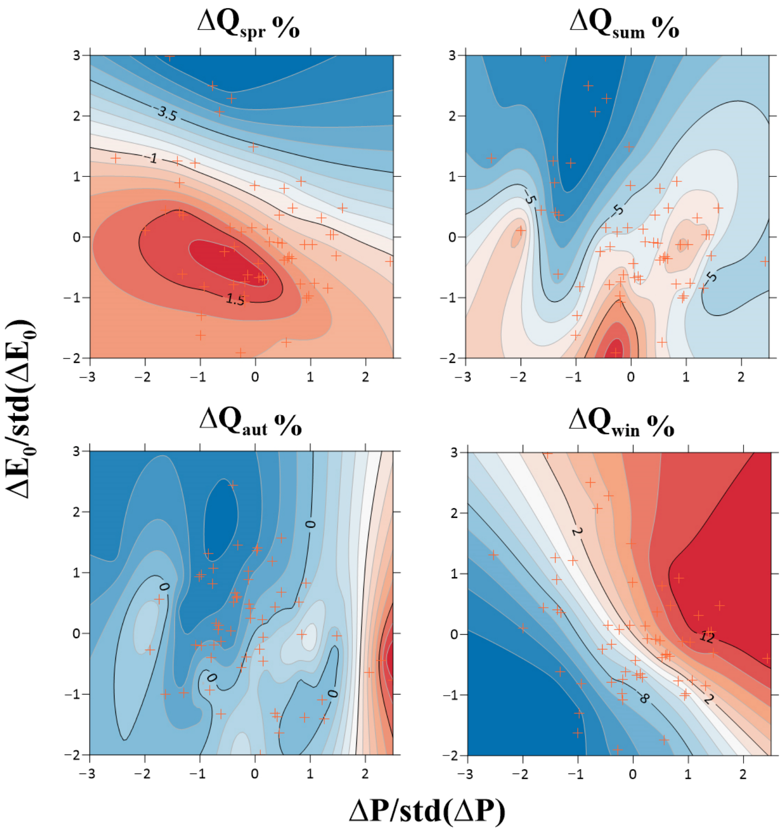

Figure 7. Contour plots of seasonal changes as a function of annual variations in precipitation (*P*) and potential evapotranspiration (E_0). Q_{spr} is the average spring runoff from 1958 to 2016; Q_{sum}, Q_{aut}, and Q_{win} are the average values of summer, autumn, and winter runoff, respectively. ΔE_0 and std(ΔE_0) are E_0 departure from the average annual E_0 and its standard deviation; ΔP and std(ΔP) are the relative changes in annual *P* to the average annual *P* and its standard deviation; ΔQ is the relative changes in seasonal runoff to their average annual values.

Figure 7 presents that the variation in autumn runoff (Q_{aut}) exhibits high sensitivity to precipitation (*P*) changes, yet it demonstrates reduced sensitivity to changes in potential evapotranspiration (E_0). Contrastingly, the spring runoff (Q_{spr}) changes are highly sensitive to E_0 alterations but are not considerably affected by changes in *P*. Notably, winter runoff (Q_{win}) displays sensitivity to both variables, while the response of summer runoff (Q_{sum}) changes to climatical variables is more complex. The evaluation of the association between the annual deviation of E_0 and the seasonal changes in *Q* shows that for every 1% enhancement in E_0, Q_{spr} decreases by 7.3%, Q_{sum} by 11.4%, and Q_{aut} by 4.6%.

4. Discussion

4.1. Climate-Driven Seasonal Runoff Dynamics

Runoff in the basin originates from four primary sources: precipitation, snowmelt, freeze–thaw processes, and ice layers beneath the frozen ground [49,50]. In recent years, the thickness of the seasonal thaw layer in frozen ground has increased by several centimetres or decimetres due to rising temperatures [51]. In small basins, the response of runoff to changes in climate factors is particularly rapid [52]. The Zhizdra River Basin, located in the central part of the East European Plain, experiences the temperate continental climate characteristic of Eastern Europe [53]. The peak runoff occurs in spring, primarily in April, while lower values are observed in summer, mainly in August. The peak in spring is caused by snowmelt, while the peak in winter is due to both snowmelt and rainfall in summer and autumn [9,54].

The significant decrease in the nonuniformity coefficient is mainly due to changes in the redistribution of runoff between the flood season and the dry season. On the one hand, the higher temperatures and increased precipitation result in a greater amount of snowmelt, leading to increased groundwater recharge and a substantial increase in river runoff during the dry season [55,56]. On the other hand, the warmer winter conditions cause a reduction in the freezing depth of the aeration zone, allowing more overland runoff to be lost through infiltration, thus significantly reducing the spring peak runoff [57].

The climate in Eastern Europe is predominantly characterized as dry or semiarid [58]. Nevertheless, the East European Plain serves as a significant agricultural region reliant on irrigation. Our analysis of Budyko framework revealed a trend towards slightly drier. This suggests that the availability of water resources restricts the basin's hydrological system. This conclusion aligns with the research conducted by Madsen, et al. [59].

Since the late 1970s, the annual average temperature has shown a significant increase, nearly double the global temperature rise, particularly during the cold season. Furthermore, precipitation has exhibited a negative trend in the warm season but a positive trend in the cold season [60,61]. Consequently, it is evident that evapotranspiration is the primary influencing factor.

4.2. Warming Enhanced the Runoff during Winter and Summer

From 1958 to 2016, the annual runoff in the Zhizdra River Basin exhibited fluctuations without a discernible trend. However, when considering seasonal variations, there was a significant increase in both summer and winter runoff ($p < 0.01$). In the Central Federal District (to which the Zhizdra Basin belongs), Volga Federal District (to the east of the Zhizdra Basin), and Northwestern Federal District (to the northeast of the Zhizdra Basin), encompassing a substantial portion of the European Russia region, this notable trend has been observed [62]. Similar increases in winter runoff and its contribution to the overall annual runoff have been observed in other prominent basins of European Russia, including the Volga River and the Don River, as well as 43% of rivers in northern Russia [60,63].

The increase in winter runoff is attributed to the rising average temperatures during the cold season (from November to April), leading to reduced snow accumulation before the onset of flooding [64]. Elevated soil temperature also contribute to a decrease in the depth of winter soil freezing, facilitating easier absorption and storage of water in the soil and subsequently augmenting runoff [65]. In addition, warming could enhance the infiltration of precipitation into the groundwater during the winter period, which not only replenishes soil moisture but also elevates the groundwater level [64]. By the early 1990s, the water level had risen by 50–130 centimetres [66].

Apart from the Zhizdra River Basin, notable increases in minimum summer runoff have also been observed in the upper reaches of the Oka River, the central part of the Volga River, and the Ural Basin [67]. The augmentation of summer runoff can be attributed to the combination of rising winter temperatures and increased precipitation, which contribute to more frequent snowmelt and reduced depth of rock freezing.

4.3. 1977, a Critical Period for the Changes in Runoff

Research indicates that the average threshold year for flow variability in Eastern Europe is 1978, which closely aligns with our study's findings [68]. Furthermore, 1977 marks a significant turning point delineating a transition between a period of relatively undisturbed natural conditions in the basin and a time when human activities and climate change intensity became more pronounced [69]. Regarding human activities, water consumption and discharge in the Russian Soviet Federative Socialist Republic (RSFSR) reached their highest levels in the late 1970s and 1980s, suggesting that human utilization and discharge of water resources had a significant impact on river flow during this period.

Additionally, the study of annual total precipitation for different types (solid, liquid, and mixed) showed a significant increase in solid and mixed precipitation after 1976. This increase, particularly in solid precipitation such as snowfall, had a significant impact on winter runoff in the region. According to the classification by M.I. Lvovich, rivers in the European territory of Russia were primarily sourced from snowmelt before the latter half of the 1970s. However, the classification changed to "mixed supply" or even "mixed supply dominated by groundwater" after 1977, indicating a shift in the sources contributing to river flow. This transition highlights the change from snowmelt dominance to a more diverse influence, including a greater impact from groundwater [70,71].

5. Conclusions

Based on the obtained results, it can be concluded that the Zhizdra River Basin has experienced significant climate changes. The annual average temperature and evapotranspiration have shown a continuous increasing trend, indicating a warming pattern in the basin. The runoff in the basin exhibited seasonal variations, with higher values during the spring, predominantly influenced by climate warming. Over time, the distribution of runoff has become more uniform, evidenced by a decrease in both the nonuniformity coefficient and concentration ratio. This suggests a more balanced and stable hydrological cycle in the Zhizdra River Basin throughout the year.

The sensitivity analysis further revealed that the runoff in the Zhizdra River Basin is more sensitive to changes in precipitation than potential evapotranspiration. Specifically, a 10% increase in precipitation resulted in a 19% increase in runoff, whereas a 10% increase in potential evapotranspiration led to a 9% decrease in runoff. These findings underscore that the basin's hydrology is primarily controlled by water availability rather than energy considerations.

Higher temperatures coupled with changes in precipitation and evapotranspiration patterns along with alterations in basin characteristics have intensified the basin's sensitivity to precipitation. Consequently, a comprehensive understanding of the hydrological responses of small river basins, particularly those with a total drainage area of less than 10,000 km^2, to a rapidly warming climate necessitates further rigorous investigation.

Author Contributions: P.W. contributed to the conceptualization and design of the study; P.W. and B.B. collected and analysed the data; Q.H., S.L. and T.W. contributed to the interpretation of the results; B.B. wrote the initial draft of the manuscript; all authors critically reviewed and revised the manuscript; P.W. and Y.Z. provided expertise and guidance; J.Y., P.W., Y.Z., S.P.P. and N.L.F. supervised the research project; all authors read and approved the final version of the manuscript; P.W. contributed to funding acquisition. All authors have read and agreed to the published version of the manuscript.

Funding: This research was funded by the National Natural Science Foundation of China (NSFC)-Russian Science Foundation (RSF) (42061134017 and 21-47-00008) and the Science & Technology Fundamental Resources Investigation Program (Grant Nos. 2022FY101900, 2022FY101901).

Data Availability Statement: The data presented in this study are available on request from the corresponding author.

Acknowledgments: The original contributions presented in the study are included in the article; further inquiries can be directed to the corresponding author. Sergey P. Pozdniakov and Ping Wang are grateful for the support of the Special Exchange Program of the Chinese Academy of Sciences (2022–2023). Muñoz Sabater, J., (2019) was downloaded from the Copernicus Climate Change Service (C3S) Climate Data Store (2022).

Conflicts of Interest: The authors declare no conflict of interest.

References

1. Yang, L.; Zhao, G.; Tian, P.; Mu, X.; Tian, X.; Feng, J.; Bai, Y. Runoff changes in the major river basins of China and their responses to potential driving forces. *J. Hydrol.* **2022**, *607*, 127536. [CrossRef]
2. Chiew, F.H.S. Estimation of rainfall elasticity of streamflow in Australia. *Hydrol. Sci. J.* **2010**, *51*, 613–625. [CrossRef]
3. Li, L.; Ni, J.; Chang, F.; Yue, Y.; Frolova, N.; Magritsky, D.; Borthwick, A.G.L.; Ciais, P.; Wang, Y.; Zheng, C.; et al. Global trends in water and sediment fluxes of the world's large rivers. *Sci. Bull.* **2020**, *65*, 62–69. [CrossRef] [PubMed]

4. Kundzewicz, Z.W.; Mata, L.J.; Arnell, N.W.; DÖLl, P.; Jimenez, B.; Miller, K.; Oki, T.; ŞEn, Z.; Shiklomanov, I. The implications of projected climate change for freshwater resources and their management. *Hydrol. Sci. J.* **2009**, *53*, 3–10. [CrossRef]
5. Dethier, E.N.; Sartain, S.L.; Renshaw, C.E.; Magilligan, F.J. Spatially coherent regional changes in seasonal extreme streamflow events in the United States and Canada since 1950. *Sci. Adv.* **2020**, *6*, eaba5939. [CrossRef]
6. Berghuijs, W.R.; Larsen, J.R.; van Emmerik, T.H.M.; Woods, R.A. A Global Assessment of Runoff Sensitivity to Changes in Precipitation, Potential Evaporation, and Other Factors. *Water Resour. Res.* **2017**, *53*, 8475–8486. [CrossRef]
7. Khaledi, J.; Lane, P.N.J.; Nitschke, C.R.; Nyman, P. Wildfire contribution to streamflow variability across Australian temperate zone. *J. Hydrol.* **2022**, *609*, 127728. [CrossRef]
8. Berghuijs, W.R.; Sivapalan, M.; Woods, R.A.; Savenije, H.H.G. Patterns of similarity of seasonal water balances: A window into streamflow variability over a range of time scales. *Water Resour. Res.* **2014**, *50*, 5638–5661. [CrossRef]
9. Pechlivanidis, I.G.; Crochemore, L.; Rosberg, J.; Bosshard, T. What Are the Key Drivers Controlling the Quality of Seasonal Streamflow Forecasts? *Water Resour. Res.* **2020**, *56*, e2019WR026987. [CrossRef]
10. Gordon, B.L.; Brooks, P.D.; Krogh, S.A.; Boisrame, G.F.S.; Carroll, R.W.H.; McNamara, J.P.; Harpold, A.A. Why does snowmelt-driven streamflow response to warming vary? A data-driven review and predictive framework. *Environ. Res. Lett.* **2022**, *17*, 053004. [CrossRef]
11. St. Jacques, J.-M.; Sauchyn, D.J. Increasing winter baseflow and mean annual streamflow from possible permafrost thawing in the Northwest Territories, Canada. *Geophys. Res. Lett.* **2009**, *36*, L01401. [CrossRef]
12. Song, C.; Wang, G.; Mao, T.; Dai, J.; Yang, D. Linkage between permafrost distribution and river runoff changes across the Arctic and the Tibetan Plateau. *Sci. China Earth Sci.* **2019**, *63*, 292–302. [CrossRef]
13. Wang, P.; Shpakova, R.N. Complex streamflow responses to climate warming in five river basins in South Yakutia, Russia. *Front. Environ. Sci.* **2022**, *10*, 1033943. [CrossRef]
14. Li, Z.; Quiring, S.M. Investigating spatial heterogeneity of the controls of surface water balance in the contiguous United States by considering anthropogenic factors. *J. Hydrol.* **2021**, *601*, 126621. [CrossRef]
15. Chen, C.; Gan, R.; Feng, D.; Yang, F.; Zuo, Q. Quantifying the contribution of SWAT modeling and CMIP6 inputting to streamflow prediction uncertainty under climate change. *J. Clean. Prod.* **2022**, *364*, 132753. [CrossRef]
16. Luo, K. Contribution of ecological conservation programs and climate change to hydrological regime change in the source region of the Yangtze River in China. *Reg. Environ. Chang.* **2022**, *22*, 10. [CrossRef]
17. Wang, M.; Zhang, Y.; Lu, Y.; Gao, L.; Wang, L. Attribution Analysis of Streamflow Changes Based on Large-scale Hydrological Modeling with Uncertainties. *Water Resour. Manag.* **2022**, *37*, 713–730. [CrossRef]
18. Aubry-Wake, C.; Pradhananga, D.; Pomeroy, J.W. Hydrological process controls on streamflow variability in a glacierized headwater basin. *Hydrol. Process.* **2022**, *36*, e14731. [CrossRef]
19. Shen, Y.; Wang, S.; Zhang, B.; Zhu, J. Development of a stochastic hydrological modeling system for improving ensemble streamflow prediction. *J. Hydrol.* **2022**, *608*, 127683. [CrossRef]
20. Herrera, P.A.; Marazuela, M.A.; Hofmann, T. Parameter estimation and uncertainty analysis in hydrological modeling. *WIREs Water* **2021**, *9*, e1569. [CrossRef]
21. Gao, H.; Zhao, F. A review of global hydrological models: The opportunities, challenges and outlook. *J. Glaciol. Geocryol.* **2020**, *42*, 224–233.
22. Sharma, P.; Mondal, A. Probabilistic Budyko-based Separation of Climate and Catchment Effects on Streamflow. *J. Hydrol.* **2022**, *608*, 127665. [CrossRef]
23. Roderick, M.L.; Farquhar, G.D. A simple framework for relating variations in runoff to variations in climatic conditions and catchment properties. *Water Resour. Res.* **2011**, *47*, W00G07. [CrossRef]
24. Dey, P.; Mishra, A. Separating the impacts of climate change and human activities on streamflow: A review of methodologies and critical assumptions. *J. Hydrol.* **2017**, *548*, 278–290. [CrossRef]
25. Lykov, I.N.; Melenchuk, V.I. Environmental problems of small rivers in the Volga and Dneprovsky basin in the territory of the Kaluga region. *IOP Conf. Ser. Earth Environ. Sci.* **2022**, *981*, 042046. [CrossRef]
26. Frolova, N.L.; Magritskii, D.V.; Kireeva, M.B.; Grigor'ev, V.Y.; Gelfan, A.N.; Sazonov, A.A.; Shevchenko, A.I. Streamflow of Russian Rivers under Current and Forecasted Climate Changes: A Review of Publications. 1. Assessment of Changes in the Water Regime of Russian Rivers by Observation Data. *Water Resour.* **2022**, *49*, 333–350. [CrossRef]
27. Borsch, S.; Simonov, Y.; Khristoforov, A.; Semenova, N.; Koliy, V.; Ryseva, E.; Krovotyntsev, V.; Derugina, V. Russian Rivers Streamflow Forecasting Using Hydrograph Extrapolation Method. *Hydrology* **2021**, *9*, 1. [CrossRef]
28. Gelfan, A.; Kalugin, A.; Millionschikova, T.; Motovilov, Y. Do changes in climatic norms influence on runoff variability? Data-based and model-based results. In Proceedings of the EGU General Assembly Conference Abstracts, Vienna, Austria, 4–13 April 2018; p. 12784.
29. Alekseevskii, N.; Lebedeva, M.Y.; Sokolovskii, D. Sources of alimentation and variability of their contribution to river runoff formation in European Russia. *Water Resour.* **2007**, *34*, 1–13. [CrossRef]
30. Semenova, I.; Morshina, T.; Semyonov, V. Impact of Anthropogenic Loads on Water Quality of Rivers of the Upper Areas of Oka and Desna Basins. In *Proceedings of the Integrated Urban Water Resources Management*; Springer: Dordrecht, The Netherlands, 2006; pp. 201–210.

31. Pozdniakov, S.P.; Grinevskiy, S.O.; Dedyulina, E.A.; Samartsev, V.N. A Model Analysis of Observed and Predicted Climatic Changes in Groundwater Recharge in a Small River Basin. *Mosc. Univ. Geol. Bull.* **2019**, *74*, 412–421. [CrossRef]
32. Pozdniakov, S.P.; Wang, P.; Grinevsky, S.O.; Frolova, N.L. A Physically Based Model of a Two-Pass Digital Filter for Separating Groundwater Runoff From Streamflow Time Series. *Water Resour. Res.* **2022**, *58*, e2021WR031333. [CrossRef]
33. Sauer, V.B.; Meyer, R. *Determination of Error in Individual Discharge Measurements*; Books and Open-File Reports Section [Distributor]; US Geological Survey: Denver, CO, USA, 1992.
34. Munoz-Sabater, J.; Dutra, E.; Agusti-Panareda, A.; Albergel, C.; Arduini, G.; Balsamo, G.; Boussetta, S.; Choulga, M.; Harrigan, S.; Hersbach, H.; et al. ERA5-Land: A state-of-the-art global reanalysis dataset for land applications. *Earth Syst. Sci. Data* **2021**, *13*, 4349–4383. [CrossRef]
35. Muñoz Sabater, J. ERA5-Land Monthly Averaged Data from 1950 to Present. Copernicus Climate Change Service (C3S) Climate Data Store (CDS). Available online: https://doi.org/10.24381/cds.68d2bb30 (accessed on 24 September 2022).
36. Du, R.; Shang, F.; Ma, N. Automatic mutation feature identification from well logging curves based on sliding *t* test algorithm. *Clust. Comput.* **2018**, *22*, 14193–14200. [CrossRef]
37. Xiao, Z.; Shi, P.; Jiang, P.; Hu, J.; Qu, S.; Chen, X.; Chen, Y.; Dai, Y.; Wang, J. The Spatiotemporal Variations of Runoff in the Yangtze River Basin under Climate Change. *Adv. Meteorol.* **2018**, *2018*, 5903451. [CrossRef]
38. Wang, X.L.; Wen, Q.H.; Wu, Y. Penalized Maximal *t* Test for Detecting Undocumented Mean Change in Climate Data Series. *J. Appl. Meteorol. Climatol.* **2007**, *46*, 916–931. [CrossRef]
39. Shine, J.M.; Koyejo, O.; Bell, P.T.; Gorgolewski, K.J.; Gilat, M.; Poldrack, R.A. Estimation of dynamic functional connectivity using Multiplication of Temporal Derivatives. *NeuroImage* **2015**, *122*, 399–407. [CrossRef]
40. Li, Z.; Wang, Y.; Guo, A.; Chang, J.; He, B.; Hu, R. Impact of intra-annual runoff nonuniformity on the energy generation of cascaded hydropower plants in Datong River Basin, China. *J. Clean. Prod.* **2021**, *323*, 129122. [CrossRef]
41. Ren, K.; Huang, S.; Huang, Q.; Wang, H.; Leng, G. Environmental Flow Assessment Considering Inter- and Intra-Annual Streamflow Variability under the Context of Non-Stationarity. *Water* **2018**, *10*, 1737. [CrossRef]
42. Xu, Z.; Liu, W.; Li, Q.; Wu, J.; Duan, H.; Huang, G.; Ge, Y. Responses of intra-annual runoff to forest recovery patterns in subtropical China. *J. For. Res.* **2020**, *32*, 1479–1488. [CrossRef]
43. Sposito, G. Understanding the Budyko Equation. *Water* **2017**, *9*, 236. [CrossRef]
44. Zhou, S.; Yu, B.; Huang, Y.; Wang, G. The complementary relationship and generation of the Budyko functions. *Geophys. Res. Lett.* **2015**, *42*, 1781–1790. [CrossRef]
45. Sinha, J.; Sharma, A.; Khan, M.; Goyal, M.K. Assessment of the impacts of climatic variability and anthropogenic stress on hydrologic resilience to warming shifts in Peninsular India. *Sci. Rep.* **2018**, *8*, 13833. [CrossRef] [PubMed]
46. Risbey, J.S.; Entekhabi, D. Observed Sacramento Basin streamflow response to precipitation and temperature changes and its relevance to climate impact studies. *J. Hydrol.* **1996**, *184*, 209–223. [CrossRef]
47. Fu, G.; Charles, S.P.; Chiew, F.H.S. A two-parameter climate elasticity of streamflow index to assess climate change effects on annual streamflow. *Water Resour. Res.* **2007**, *43*, W114119. [CrossRef]
48. Wang, P.; Huang, Q.; Pozdniakov, S.P.; Liu, S.; Ma, N.; Wang, T.; Zhang, Y.; Yu, J.; Xie, J.; Fu, G.; et al. Potential role of permafrost thaw on increasing Siberian river discharge. *Environ. Res. Lett.* **2021**, *16*, 034046. [CrossRef]
49. Wang, G.; Hu, H.; Li, T. The influence of freeze–thaw cycles of active soil layer on surface runoff in a permafrost watershed. *J. Hydrol.* **2009**, *375*, 438–449. [CrossRef]
50. Bazarzhapov, T.Z.; Shiretorova, V.G.; Radnaeva, L.D.; Nikitina, E.P.; Sodnomov, B.V.; Tsydypov, B.Z.; Batomunkuev, V.S.; Taraskin, V.V.; Dong, S.; Li, Z.; et al. Trend Analysis of Precipitation, Runoff and Major Ions for the Russian Part of the Selenga River Basin. *Water* **2023**, *15*, 197. [CrossRef]
51. Frauenfeld, O.W. Interdecadal changes in seasonal freeze and thaw depths in Russia. *J. Geophys. Res.* **2004**, *109*, D05101. [CrossRef]
52. Kalyuzhnyi, I.L.; Lavrov, S.A. Basic physical processes and regularities of winter and spring river runoff formation under climate warming conditions. *Russ. Meteorol. Hydrol.* **2012**, *37*, 47–56. [CrossRef]
53. Cheval, S.; Dumitrescu, A.; Birsan, M.-V. Variability of the aridity in the South-Eastern Europe over 1961–2050. *Catena* **2017**, *151*, 74–86. [CrossRef]
54. Liu, S.; Wang, P.; Yu, J.; Wang, T.; Cai, H.; Huang, Q.; Pozdniakov, S.P.; Zhang, Y.; Kazak, E.S. Mechanisms behind the uneven increases in early, mid- and late winter streamflow across four Arctic river basins. *J. Hydrol.* **2022**, *606*, 127425. [CrossRef]
55. Godsey, S.E.; Kirchner, J.W.; Tague, C.L. Effects of changes in winter snowpacks on summer low flows: Case studies in the Sierra Nevada, California, USA. *Hydrol. Process.* **2014**, *28*, 5048–5064. [CrossRef]
56. Allen, D.M.; Cannon, A.J.; Toews, M.W.; Scibek, J. Variability in simulated recharge using different GCMs. *Water Resour. Res.* **2010**, *46*, W00F03. [CrossRef]
57. Dzhamalov, R.G.; Frolova, N.L.; Krichevets, G.N.; Safronova, T.I.; Kireeva, M.B.; Igonina, M.I. The formation of present-day resources of surface and subsurface waters in European Russia. *Water Resour.* **2012**, *39*, 623–639. [CrossRef]
58. Nistor, M.-M. High-resolution projections of the aridity in Europe under climate change. In *Climate and Land Use Impacts on Natural and Artificial Systems*; Elsevier: Amsterdam, The Netherlands, 2021; pp. 73–90.
59. Madsen, H.; Lawrence, D.; Lang, M.; Martinkova, M.; Kjeldsen, T.R. Review of trend analysis and climate change projections of extreme precipitation and floods in Europe. *J. Hydrol.* **2014**, *519*, 3634–3650. [CrossRef]

60. Dzhamalov, R.G.; Safronova, T.I.; Telegina, E.A. Annual distribution of river runoff with estimated contribution of winter low-water season. *Water Resour.* **2017**, *44*, 785–792. [CrossRef]
61. Huang, Q.; Liu, S.; Wang, P.; Wang, T.; Yu, J.; Chen, X.; Yang, L. Spatiotemporal variability of temperature and precipitation in typical Pan-Arctic basins, 1936–2018. *Resour. Sci.* **2020**, *42*, 2119–2131. [CrossRef]
62. Shiklomanov, I.A.; Babkin, V.I.; Balonishnikov, Z.A. Water resources, their use, and water availability in Russia: Current estimates and forecasts. *Water Resour.* **2011**, *38*, 139–148. [CrossRef]
63. Kireeva, M.; Frolova, N.; Rets, E.; Samsonov, T.; Entin, A.; Kharlamov, M.; Telegina, E.; Povalishnikova, E. Evaluating climate and water regime transformation in the European part of Russia using observation and reanalysis data for the 1945–2015 period. *Int. J. River Basin Manag.* **2020**, *18*, 491–502. [CrossRef]
64. Barabanov, A.T.; Dolgov, S.V.; Koronkevich, N.I.; Panov, V.I.; Petel'ko, A.I. Surface Runoff and Snowmelt Infiltration into the Soil on Plowlands in the Forest-Steppe and Steppe Zones of the East European Plain. *Eurasian Soil Sci.* **2018**, *51*, 66–72. [CrossRef]
65. Gusarov, A.V. The impact of contemporary changes in climate and land use/cover on tendencies in water flow, suspended sediment yield and erosion intensity in the northeastern part of the Don River basin, SW European Russia. *Environ. Res.* **2019**, *175*, 468–488. [CrossRef]
66. Serykh, I.V.; Kostianoy, A.G. The Links of Climate Change in the Caspian Sea to the Atlantic and Pacific Oceans. *Russ. Meteorol. Hydrol.* **2020**, *45*, 430–437. [CrossRef]
67. Sidorchuk, A.Y.; Panin, A.V.; Borisova, O.K. Morphology of river channels and surface runoff in the Volga River basin (East European Plain) during the Late Glacial period. *Geomorphology* **2009**, *113*, 137–157. [CrossRef]
68. Dzhamalov, R.; Frolova, N.; Telegina, E. Winter runoff variations in European Russia. *Water Resour.* **2015**, *42*, 758–765. [CrossRef]
69. Magritskii, D.V. Anthropogenic impact on the runoff of Russian rivers emptying into the Arctic Ocean. *Water Resour.* **2008**, *35*, 1–14. [CrossRef]
70. Frolova, N.; Kireeva, M.; Nesterenko, D.; Agafonova, S.; Tersky, P. Up-to-date climate forced seasonal flood changes (the case study for European part of Russia). *IAHS Publ.* **2014**, *363*, 113–118.
71. Dzhamalov, R.G.; Frolova, N.L.; Rets, E.P.; Bugrov, A.A. Formation of current groundwater resources in European Russia. *Water Resour.* **2015**, *42*, 563–571. [CrossRef]